L JAST
Libya Journal Applied For Science and Technology
مجلة ليبيا للعلوم التطبيقية والتقنية

Volume 5.Issue1
December2018

Study of a Complex Rheometric Device for Determination of Pressure Dependent Viscosity

Ahmed S. El maalul[1], M. A. Nwir[2], M Alhajaji[2]

[1]Dept. of Mechanical Engineering, Tripoli University

[2]Dept. of Mechanical Engineering, College of Technical Engineering-Janzour

Abstract

Hydrodynamic pressure technique is a relatively new and innovative technique for rheological studies of viscous non-Newtonian fluids. These principles have been extensively used for the last twenty years for drawing and coating of strips and wires. The Rheometric Device consists of a rotating inner cylinder (rod) in a fixed hollow outer cylinder. The complex geometry gap between the two cylinders is filled with a viscous non-Newtonian fluid. When the rod rotates inside, while the hollow cylinder filled with a viscous fluid, shearing takes place and hydrodynamic pressure develops, the magnitude of which is dependent on the shape of the surfaces, the viscosity of the fluid as well as the shear rate , the speed with which the inner solid rod is rotating. The rheometer has been developed to determine the Rheological properties of viscous fluid at pressures of *up to 100 bar* and a shear rate range of $500\ to 400\ sec^{-1}$.

theoretical models have been developed based on the non-Newtonian characteristics and a shear rate viscosity relationship was determined using the rheometer at different pressures by comparing the calculated theoretical pressure distribution with the experimental results.

Keywords: Non-Newtonian fluid, polymer, rotate speed, shear rate viscosity.

1. Introduction

Rheology is a general term for the study of deformation and flow of materials , it originates from the Greek word “rhein”, which means, “to flow” rheology is concerned with the flow and deformation of materials experiencing an applied force [1]. This definition was accepted when the American Society of

rheology , the scope is even wider Significant advances have been made in bio rheology, in polymer rheology and suspension rheology There has also been a significant appreciation of the importance of rheology in chemical processing industries [1]. rheology was founded in 1929. That first meeting heard papers on the properties and behavior of such widely differing materials as asphalt, lubricants, paints, plastics and rubber, which gives some idea of the scope of the subject and also the numerous scientific disciplines likely to be involved [2-3] . Opportunities no doubt exist for more extensive applications of rheology in the biotechnological industries rheology is becoming more and more important in plastic industry [4-7], both in areas of development and processing , Other applications of rheology are as follows: (i) Pumping slums-materials transport (ii) Thickening and de-watering of mineral slurries. (iii) Filtration. (iv) Forming materials (e.g. brick and ceramic products). (v) Paint manufacture (e.g. non-drip paints) (vi) Reactions involving

mineral slurries (e.g. gold extraction). (vii) Food chemistry and manufacture-texture of ice cream, pasta, desserts, processed meats, cosmetics chemistry. (viii) Drilling mud for petroleum industry. (ix) Polymer chemistry-solution and melts. (x) Plasto-hydrodynamic wire drawing and wire coating rheological properties required for good coating performance[8]. In recent studies of thermoplastic injection molding, sophisticated rheological techniques have been employed to characterize the viscous behavior since the findings of rheology are of fundamental importance for the development, manufacture and processing of innumerable products[9]. Without rheology, nothing in materials and process engineering can have function today Rheometry is the technology, which involves the rheological measurement of fluids. The flow characteristics of non-Newtonian fluids are influenced by many factors, which are described m relation to the present work for developing a new type of rheometer for rheological studies of glycerin, silicone, liquid honey, polymer melt etc.

2. Analysis:

Analysis were based on the geometrical configuration shown in the Figure (1) .And the following assumptions were made:

1- The flow of polymer melt is axial and laminar.
2- Thickness of the polymer melt layer is small compared to the unit dimensions.
3- shear stress in the polymer melt is assumed to be constant for a constant drawing speed.
4- fluid has the characteristics of a non-Newtonian fluid, namely, the viscosity is dependent on the shear rate and pressure.

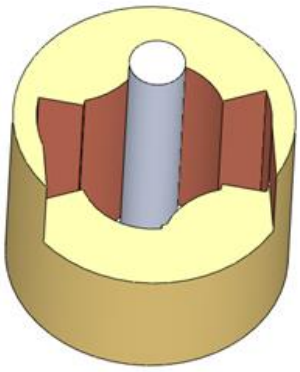

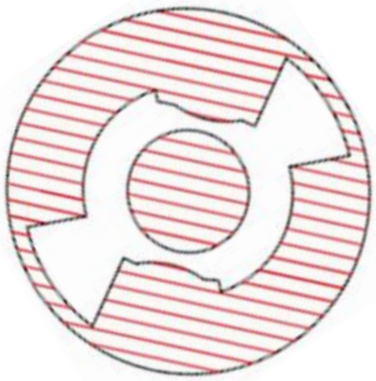

Fig. 1 combined pressure unit (parallel and hyperbolic bore)

2.1. Determination of pressure within the unit

Plasto-hydrodynamic pressure model within the first part of the unit (parallel part)

Two different equations are generally used to express the shear stress and shear rate relation for a polymer solution. The first is a power law equation given by.

$$\tau = \mu\left(\frac{du}{dy}\right)^n \quad (1)$$

This equation is applicable for any type of fluid . Here n is the power law index which equals to (1) for non-Newtonian fluid, greater than (1) for dilettante fluid and less than (1; 0) for pseudo plastic fluid. In this equation τ is the shear stress, μ is the viscosity.

The relationship between the pressure and the shear stress gradient in the first part of the unit is given by,

$$\left(\frac{dp}{dx}\right)_1 = \left(\frac{d\tau}{dy}\right)_1 \quad (2)$$

$$\tau_1 + k\tau_1^3 = \mu(\frac{du}{dy}) \quad (3)$$

Considering Figure (1), the steady state flow of polymer is given by equation (2) in which after integration w.r.to y gives:

$$\left(\frac{dp}{dx}\right)_1 y + C_1 = \tau_1 \,,\ \tau_1 = p_1' y + c_1 \quad (4)$$

Where: *C1* is a constant.

$p' = (dp/dx)$

At the surface of the wire $y = 0$ and $\tau_1 = \tau_{c1}$ so that,

$$\left(\frac{dp}{dx}\right)_1 y + \tau_{c1} = \tau_1 \quad (5)$$

Substituting for τ_1 from equation (3) into equation (5) gives,

$$\mu\left(\frac{du_1}{dy}\right) = \left(\frac{dp_1}{dx}\right) y + \tau_{c1} + k[\left(\frac{dp_1}{dx}\right) y + \tau_{c1}]^3$$

Integration of the above equation w.r.to y gives,

$$\mu u_1 = \left(\frac{dp_1}{dx}\right)\frac{y^2}{2} + \tau_{c1} y + k(Q) + C_2 \quad (6)$$

Where : C_2 is constant,

$$Q = [(\frac{dp_1}{dx})^3 \frac{y^4}{4} + (\frac{dp_1}{dx})^2 y^3 \tau_{c1} + (\frac{dp_1}{dx})\frac{3y^2\tau_{c1}^2}{2} + \tau_{c1}^3 y]$$

The boundary conditions at speeds at which slip does not occur are,

(a_1)- at wire surface $y = 0$, $u_1 = v_1$

(b_1)- at the unit surface $y = h_1$, $u_1 = 0$

Where V is the velocity of the undeformed wire. Substituting condition, (a_1) into the above equation, $V = C_2/\mu$

So that,

$$u_1 = \left(\frac{dp_1}{dx}\right)\frac{y^2}{2\mu} + \frac{\tau_{c1}}{\mu} y + \frac{k}{\mu}[(\frac{dp_1}{dx})^3 \frac{y^4}{4} + (\frac{dp_1}{dx})^2 y^3 \tau_{c1} + (\frac{dp_1}{dx})\frac{3y^2\tau_{c1}^2}{2} + \tau_{c1}^3 y] + V \quad (7)$$

Applying the boundary conditions (b1) to find τc1 at the surface of the pressure unit,

$$0 = (\frac{dp_1}{dx})\frac{h_1^2}{2\mu} + \frac{\tau_{c1} h_1}{\mu} + \frac{k}{\mu}[(\frac{dp_1}{dx})^3 \frac{h_1^4}{4} + (\frac{dp_1}{dx})^2 h_1^3 \tau_{c1} + (\frac{dp_1}{dx})\frac{3h_1^2\tau_{c1}^2}{2} + \tau_{c1}^3 h_1] + V$$

Rearranging the above equation in terms of the power of τ_{c1}

$$\tau_{c1}^3 + (\frac{dp_1}{dx})\frac{3h_1\tau_{c1}^2}{2} + \tau_{c1}[\frac{1}{k} + (\frac{dp_1}{dx})^2 h_1^2] + [(\frac{dp_1}{dx})\frac{h_1}{2k} + (\frac{dp_1}{dx})^3 \frac{h_1^3}{4} + \frac{\mu v}{k h_1}] = 0$$

After solving

$$\tau_{c1} = (-\frac{\mu v}{2k h_1} + [\frac{\mu^2 v^2}{4k^2 h_1^2} + \frac{1}{27}(\frac{1}{k} + (\frac{dp_1}{dx})^2 \frac{h_1^2}{4})^3]^{\frac{1}{2}})^{\frac{1}{3}}$$

$$+(-\frac{\mu v}{2k h_1} - [\frac{\mu^2 v^2}{4k^2 h_1^2} + \frac{1}{27}(\frac{1}{k} + (\frac{dp_1}{dx})^2 \frac{h_1^2}{4})^3]^{\frac{1}{2}})^{\frac{1}{3}}$$

$$-\frac{h_1}{2}(\frac{dp_1}{dx}) \quad (8)$$

The above equation gives the shear stress on the wire before deformation for known values of (dp/dx). The flow of liquid polymer in the axial direction within the gap before the step may be given by,

$$Q_1 = \int_0^{h_1} u_1 \, dy$$

Substituting for u_1 into the above equation (7) and integrating,

$$Q_1 = \left(\frac{dp_1}{dx}\right)\frac{h_1^3}{6\mu} + \frac{\tau_{c1} h_1^2}{2\mu} + \frac{k}{\mu}[(\frac{dp_1}{dx})^3 \frac{h_1^5}{20} +$$

$$\left(\frac{dp_1}{dx}\right)^2 \frac{h_1^4 \tau_{c1}}{4} + \left(\frac{dp_1}{dx}\right)\frac{h_1^3 \tau_{c1}^2}{2} + \frac{\tau_{c1}^3 h_1^2}{2}\Bigg] + Vh_1 \quad (9)$$

The flow of liquid polymer obey the continuity equation so that,

$$\frac{dQ_x}{dx} + \frac{dQ_y}{dy} + \frac{dQ_z}{dz} = 0$$

Under axial and laminar flow conditions,

$$\frac{dQ_y}{dy} = \frac{dQ_z}{dz} = 0$$

And hence,

$$\frac{dQ_x}{dx} = 0$$

Substituting for τc_1 from equation (8) into equation (9) and nothing that h_1 ,μ and V are constants and that $(dQx/dx) = 0$, it is shown that,

$$\left(\frac{dp_1}{dx}\right) = \frac{P_{step}}{L_1} = \text{Constant}$$

Where :

P_{step} is the pressure at the step and L_1 is the length of the first part of the unit. Thus the pressure profile in the first part of the unit is linear. However, P_{step} cannot be determined at this stage since equation (9) contains the unknown variable Q_1 and it must be defined.

Plasto-hydrodynamic pressure model within the 2nd part (The Converging hyperbolic) , Figure (2)

Equation (9) can be written as:

$$Q = \frac{(dp/dx)h^3}{12\mu} - \frac{K}{\mu}\left(\frac{\tau^2 (dp/dx)h^3}{4}\right) + V\frac{h}{2} \quad (10)$$

Considering a position where $h = h_b$, the pressure is maximum. Therefore in that position $(dp/dx) = 0$ which gives $(Q = Vh_b/2)$

Thus,

$$\frac{dp}{dx} = \frac{6\mu v}{[1 + 3k\tau^2]}\left[\frac{1}{h^2} - \frac{h_b}{h^3}\right]$$

The boundary conditions are,

with the boundary condition (at x=0 & P=0) the pressure expression becomes:

$$P(x) = \frac{6\mu V}{[1 + 3K\tau^3]}[H(x) - h_b G(x)]$$

With the boundary condition (at x=L & P=0) the position of optimum pressure is:

$h_b = H(L) - G(L)$

Therefore, the pressure profile in this part is :

$$P(x) = \frac{6\mu V}{[1 + 3K\tau^3]}\left[H(x) - \frac{H(L)G(x)}{G(L)}\right] \quad (11)$$

For converging parabolic shape , the geometry of the unit can be considered as ,

$$h(x) = -a^2 (x + b)^2 + c^2$$

substituting $h(x)$ in the expression for $H(x)$ it becomes,

$$H(x) = \int_0^x \frac{1}{(-a^2(x + b)^2 + c^2)^2}\, dx$$

After integration it becomes,

$$H(x) = \frac{1}{4C^3 a}\left[\ln\left[\frac{x + b + d}{x + b - d}\right] - \ln\left[\frac{b + d}{b - d}\right] - d[Q']\right]$$

$$Q' = \frac{1}{x + b + d} + \frac{1}{x + b - d} - \frac{1}{b + d} - \frac{1}{b - d} \quad (12)$$

And in the same way substituting $h(x)$ in the expression for $G(x)$, it gives

$$G(x) = \int_0^x \frac{1}{(-a^2(x + b)^2 + C^2)^3}$$

After integration it gives,

$$G(x) = \frac{1}{16d^5a^6}\left[3\ln\left[\frac{x+b+d}{x+b-d}\right] - 3\ln\left[\frac{b+d}{b-d}\right]\right.$$

$$-(A) - (Z) \qquad (13)$$

Where:

$$A = 3d\left[\frac{1}{x+b+d} + \frac{1}{x+b-d} - \frac{1}{b+d} - \frac{1}{b-d}\right]$$

$$Z = d^2\left[\frac{1}{(x+b+d)^2} - \frac{1}{(x+b-d)^2} - \frac{1}{(b+d)^2} + \frac{1}{(b-d)^2}\right.$$

Where, d = c/a

To obtain the optimum position for pressure , it is necessary to calculate G(L) and H(L) for hydrodynamic converging parabolic part, where the second part geometry can be expressed as:

$$h(x) = -\left(h_1 - \frac{h_2}{L}\right)X^2 + h_1$$

Therefore in this case substitution for:

$$b=0 \quad , \quad c = \sqrt{h_1} \quad , \quad a = \frac{\sqrt{h_1-h_2}}{L}$$

Substituting the values for a, b and c at x=L , the expression for G(L) and H(L) becomes :

$$G(L) = \frac{L}{16h_1^2\sqrt{h_1}\sqrt{h_1-h_2}}\left[3\ln\frac{\sqrt{h_1-h_2}+\sqrt{h_1}}{\sqrt{h_1-h_2}-\sqrt{h_1}} - 3d\left(\frac{2L}{L^2-d^2} + d^2\left(\frac{4Ld}{(L^2-d^2)}\right)\right)\right]$$

Therefore,

$$G(L) = \frac{L}{16h_1^2\sqrt{h_1}\sqrt{h_1-h_2}}\left[3\ln\frac{\sqrt{h_1-h_2}+\sqrt{h_1}}{\sqrt{h_1-h_2}-\sqrt{h_1}}\right] + \frac{1}{16h_1}\left[\left(\frac{6L}{h_1h_2} + \frac{4L}{h_2^2}\right)\right] \qquad (14)$$

In the same way,

$$H(L) = \frac{L}{4h_1\sqrt{h_1}\sqrt{h_1-h_2}}\left[\ln\frac{\sqrt{h_1-h_2}+\sqrt{h_1}}{\sqrt{h_1-h_2}-\sqrt{h_1}}\right] + \frac{L}{2h_1h_2} \qquad (15)$$

3. Predicted Results.

Theoretical results were obtained using the equations derived in the theoretical analysis section. The following are the magnitudes of known parameters which were used to solve the equations and were varied to shows their effect on the pressure distribution in the unit. Table (1) shown the Dimension of the system.

Where :

Angular speed ω " rad/s" & Liner speed v = ω * D/2.

Table 1 : Dimension of the system

	Description	Code	Value
1	Length of the first part of the unit	L_1	60 (mm)
2	Length of the parabolic part of the unit	L_2	20 (mm)
3	Gap at the entry end of the unit	h_1	1 (mm)
4	Gap at the step	h_2	0.5 (mm)
5	Gap at the exit end of the unit	h_3	0.05 (mm)
6	Reference Viscosity	μ	100N.s/ m²
7	Diameter	D	20 (mm)

Fig. 2 Dimension of the die (parallel and hyperbolic bore)

3.1. Predications for maximum pressure

Figures (3) shows the effect of h_1 , h_2 & h_3 respectively on maximum pressure. These figures indicate smaller values of h_1 , h_2 & h_3 the maximum pressure is increased for a given drawing speed. This figure show that change in the

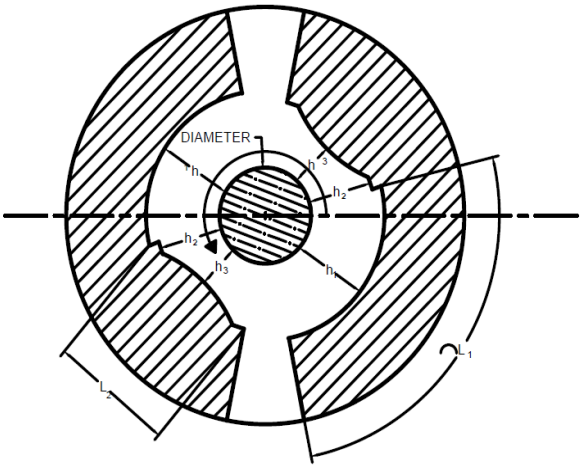

values of h_3 have more effect than on both of h_1 , h_2 on the maximum pressure. Figure (4) shows effect on the maximum pressure. This figure indicates that when the viscosity of polymer increases, the maximum pressure increased for a given drawing speeds..

The effect of the length of L_1 & L_2 of the unit on maximum pressure are illustrated in figures.

Figure (5) shows the values change of L_2 , the maximum pressure should increase at all drawing speeds.

3.2.Predictions for Pressure Distribution Change of h_2 values

Figures (6) shows the theoretical pressure distribution for two different gap ratios. Figure (6) shows the pressure distribution for gap ratio of $h_2/h_3 = 10$ when $h_2 = 0.0005m$, $h_3 constant = 0.00005$ m. at three different drawing speeds. $(\omega_1 = 25$, $\omega_2 = 45$ And $\omega_3 = 65)$rad /s. At gap ratio of $h_2/h_3 = 20$, when $h_2 = 0.0007$ m

$h_3 constant = 0.00005\, m.$ at three different drawing speeds, $(\omega_1 = 25$, $\omega_2 =$ s And $\omega_3 = 65)$rad /s.

When the gap ratio of $h_2/h_3 = 30$, when $h_2 =$ 0.0009 m , $h_3$constant $= 0.00005$ m. at three different drawing speeds. $(\omega_1 = 25$, $\omega_2 =$ 45 And $\omega_3 = 65)$rad /s.

4. Discussion of Pressure Results.

The pressure unit consists of combined both parallel and parabolic bores. To investigate the performance of the unit, a simulation program was conducted during which a considerable amount of data were obtained.

The results of the pressures are divided into two sections:

1) Maximum pressure *Vs.* " ω " speed.
2) The pressure profiles along the length (pressure distribution).

4.1. Results of Maximum Pressure Vs. Speed.

In order to determine the optimum condition for which the magnitude of maximum Pressure is predicted figures (3) show the effect of h_1 , h_2 & h_3 respectively on maximum pressure. This figure indicates that for smaller values of h_1 , h_2 & h_3 , the maximum pressure increases when the drawing speed increased also, and when the values of h_1 , h_2 & h_3 increases the maximum pressure values decreased. Thus the change in the value of h_3 has comparatively greater than of h_1 , h_2 on the maximum pressure.

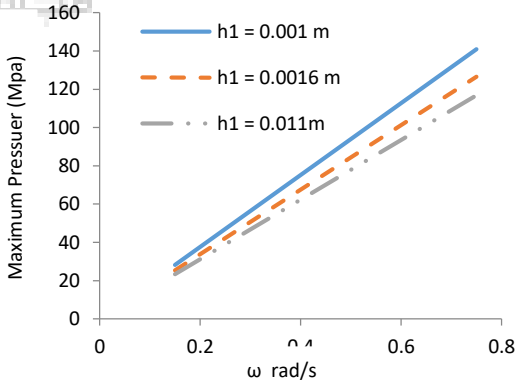

Fig. 3 Theoretical effect of h_1 on Maximum pressure

Figure (4) shows effect of viscosity on the maximum pressure. This figure indicates that when the viscosity of polymer increases the maximum pressure increased for a given drawing speeds and when the value of viscosity polymer increases the maximum pressure value also increased for a given drawing speed.

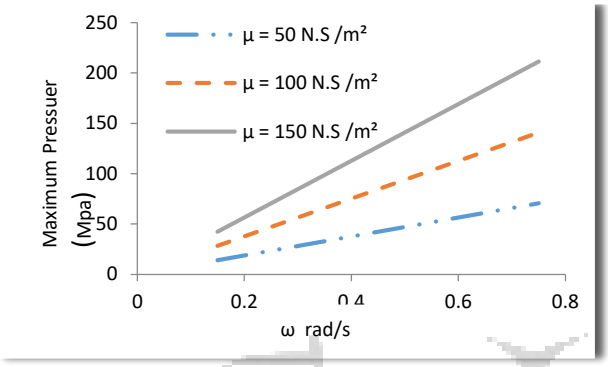

Fig. 4 Theoretical effect of viscosity " μ " on Maximum pressure

The maximum pressure increases when the drawing speed value increased, however, the change values of L_2 the maximum pressure should increase at all drawing speeds. And the pressure maximum increases when L_1 & L_2 values are increased.

4.2. Results of Pressure Distribution

Pressure distribution within the stepped gap pressure unit, based on experimentally measured pressure at two different locations, one in the middle of the first insert part L_1 of the unit and the other in the middle of the second insert part L_2 of the unit, have been obtained and plotted for the gap ratio h_2/h_3 = 10 ,20 and 30 when h_3 constant = 0.00005 m .

Figure (5) shows pressure distribution for gap ratio h_2/h_3 =10 when $h_2 = 0.0005\text{m}$. at three different drawing speeds. ($\omega_1 = 25$, $\omega_2 = 45$ And $\omega_3 = 65$)rad /s.

This figure suggests that the pressure increased from zero at the entry of the unit to maximum value when at x = 0.075 m for all above speed values, however the most value obtained at $\omega_3 = 65$ rad/s. The pressure increases as the drawing speed increased. The maximum pressure was 122 MPa.

The pressure distribution for gap ratio h_2/h_3 =20 when $h_2 = 0.001\text{m}$. at three different drawing speeds. the pressure increases up gradually to maximum pressure value a $x = 0.078\text{m}$. For all above speed values and the maximum pressure were found when drawing speed $\omega_3 = 65$ rad/s . 93 MPa

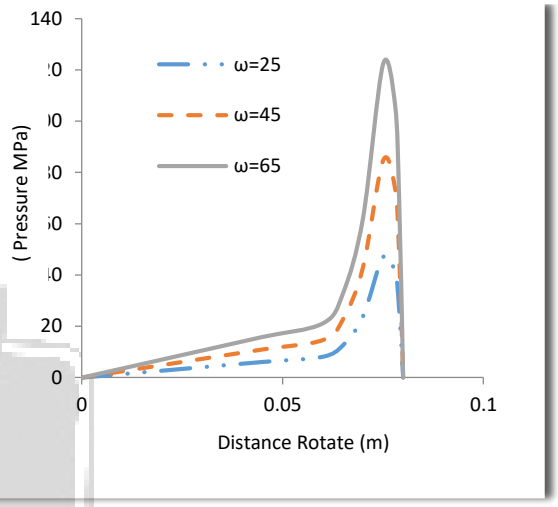

Fig. 5 Results of pressure distribution at $h_2/h_3 = 10$

In the gap ratio h_2/h_3 =30 when $h_2 = 0.0015\text{m}$. at three different drawing speeds. Pressure increases up gradually to maximum pressure value at $x = 0.078$ m . For all above speed values and the maximum pressure was found equal to 89 MPa when drawing speed $\omega_3 = 65$ rad/s .

Also the change of gap ratio h_2/h_3 does not affect the pressure distribution in the first part of the unit. The effect of length ratio on pressure distribution is illustrated the pressure distribution for two different length ratios L_1/L_2 = 3 & L_1/L_2 = 3.25 at the drawing speed of $\omega_1 = 25$ rad/s . At L_2 constant = 0.02 m (20mm) .

Figure (6) shows the pressure distribution for two different length ratios for L_1/L_2 = 3 & L_1/L_2 = 2.4 the drawing speed of $V_1 = 0.25$ m/s . At L_1 constant = 0.06 m (60mm) , this figure suggests that the maximum pressure increases, as length ratio is increased for a given drawing speed. The pressure was: (60 MPa at $\omega_1 = 25$ rad/s , x = 0.08m).

4.3.Effect the gap ratio with angular speed.

The Figure (7) shows pressure was increased when the gap ratio changed. The study focused on selecting the change in gap ratio $^{h_2}/_{h_3}$ because they were the most influential in the distribution of pressure. therefore, the maximum pressure value occurred when the lowest value for h_2 and the lowest value for h_3 .

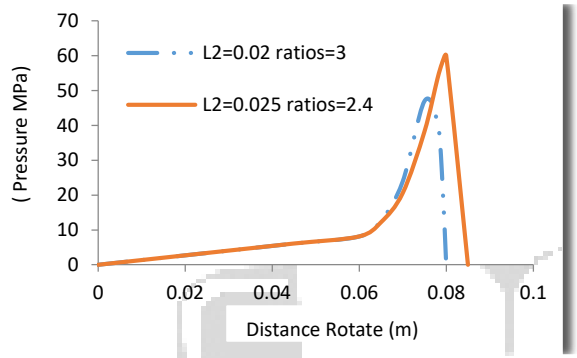

Fig. 6 pressure distribution with change value of L_2

Where :

$h_2 = 0.0005$ m, $h_3 = 0.00005$ m. It was 140 MPa.

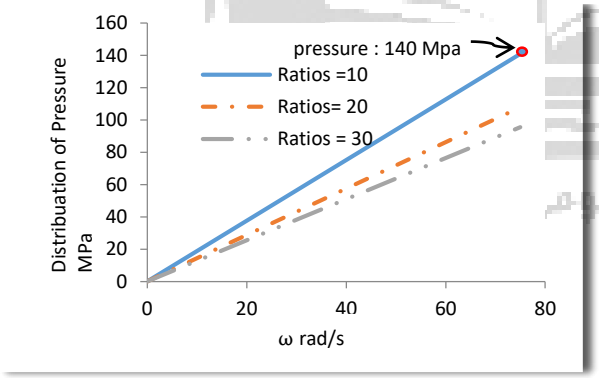

Fig. 7 pressure distribution with change gap ratio $\boldsymbol{h_2}$&$\boldsymbol{h_3}$

5.Effect of shear rate on the viscosity.

The effect of shear rate on viscosity is presented in Figure (8) From the figure the viscosity increases with the decrease of shear rate.

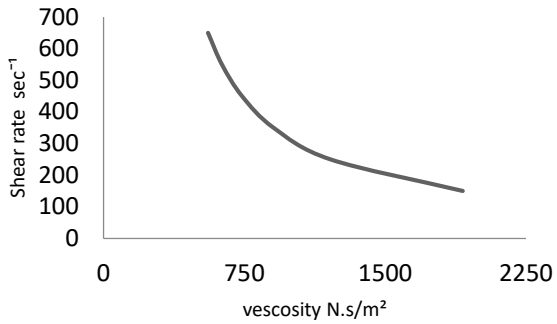

Fig. 8 Effect of shear rate on viscosity

5. Conclusion

In this study , a theoretical analysis based on the non-Newtonian fluid characteristics has been developed. Hydro-dynamic pressure units could be usefully for a number of possible applications such as drawing processes, coating of wires, tubes, ropes and wire-ropes and viscosity measuring for different types of fluids.

Based on the theoretical results obtained for the mentioned Rheometric unit, it may be concluded that there exists an optimum value for the gap ratio which will generate the greatest magnitude of pressure , effect of pressure on viscosity also included as well as the gaps of the unit, the unit could be used for viscosity measurements knowing the pressure generated values and the unit dimensions helps in predicting the viscosity.

References

[1] S. Akter, M.S.J. Hashmi, Wire drawing and coating using a combined geometry hydrodynamic unit: Theory and experiment ,Journal of Materials Processing Technology, Volume 178.1-3,14 September 2006,pp98-110.

[2] RABINOWITSCH B, Uber die viskostat und elastizitzt von solen, Z. Phys. Chem.1929, A145, pp 141.

[3] Akhter, Salma " Development of a novel Rheometric device for the determination of pressure dependent viscosity of non-Newtonian fluids", Master of Engineering thesis, Dublin City University, Ireland.

[4] S.Akter,M S J Hashmi, Hydrodynamic wire coating using tapered bore pressure unit, journal of Material Processing Technology-T MATER process Technol.01/2006,174(1) pp 348-388.

[5] S.Akter, M S J Hashmi., Modeling of pressure distribution within hydrodynamic pressure unit: effect of the change in viscosity during drawing of wire coating, Journal of Materials Processing Technology, vol.77,Number 1,May 1998,pp 32-36(5).

[6] M. A Nwir, M S J Hashmi, A non-Newtonian plasto-hydrodynamic modeling of pressure distribution using tapered bore unit, AL-Jufra journal of science and engineering, vol.1,No(1) ,October 2001,Libya.

[7] M. A Nwir, M S J Hashmi., Plasto-hydrodynamic pressure distribution in a complex geometry pressure unit: experimental results using Borosiloxane as pressure medium, IMC 11, The Queens University of Belfast, August/September 1994, Ireland.

[8] H. A .Barnes , J. F. Hutton and K. Walter F .R. S, An introduction to Rheology , Amsterdam-London-New York-Tokyo, page 20.

[9] M.A Nwir, A.A Alaojily, Plasto-Hydrodynamic Pressure Modeling Using a Converging Parabolic Coating Unit, Theoretical Predictions, Journal of applied Science & Engineering Research, College of Engineering Technology ,Houn.15.

[10] Ahmed S. El maalul, M. A. Nwir, M. Alhaji, Plasto-hydrodynamic Modeling of Pressure Distribution Using Complex Shaped Unit, H.A. R. jennah ,Theoretical Predictions, Vol. 1,No.1,2017. Libya.

[11] Samia M. Jumma , M.A. Nwir , Mustafa Alhajaji, "Plasto-Hydrodynamic Pressure Modeling Using a Converging Parabolic Coating Unit", Theoretical Predictions., , Journal of Engineering Research & Applied Science (JERAS) 4th Edition, December 2017, Volume .1, Hoon Libya.